

---

# JOURNAL OF THE AMERICAN CHEMICAL SOCIETY

---

## Kinetic Analysis of a Protein Tyrosine Kinase Reaction Transition State in the Forward and Reverse Directions

Kyonghee Kim and Philip A. Cole\*

Contribution from the Laboratory of Bioorganic Chemistry, Rockefeller University,  
New York, New York 10021

Received March 13, 1998

**Abstract:** Protein tyrosine kinases catalyze the transfer of the  $\gamma$ -phosphoryl group from ATP to tyrosine residues in proteins and are important enzymes in cell signal transduction. We have investigated the catalytic phosphoryl transfer transition state of a protein tyrosine kinase reaction catalyzed by Csk by analyzing a series of fluorotyrosine-containing peptide substrates. It was established for five such fluorotyrosine-containing peptide substrates that there is good agreement between the tyrosine analogue phenol  $pK_a$  and the ionizable group responsible for the basic limb of a pH rate profile analysis. This indicates that the substrate tyrosine phenol must be neutral to be enzymatically active. Taken together with previous data indicating a small  $\beta_{\text{nucleophile}}$  coefficient (0–0.1), these results strongly support a dissociative transition state for phosphoryl transfer. In addition, the  $\beta_{\text{leaving group}}$  coefficient was measured for the reverse protein tyrosine kinase reaction and shown to be  $-0.3$ . This value is in good agreement with a previously reported nonenzymatic model phosphoryl transfer reaction carried out under acidic conditions (pH 4) and is most readily explained by a transition state with significant proton transfer to the departing phenol.

Protein tyrosine kinases catalyze the transfer of the  $\gamma$ -phosphoryl group of ATP to proteins on tyrosine residues (Figure 1). These enzymes are critical for cell signal transduction in a variety of physiologic contexts.<sup>1</sup> Because of their importance in embryonic development, cancer, neurobiology, endocrinology, and immunology, protein tyrosine kinases have been intensively

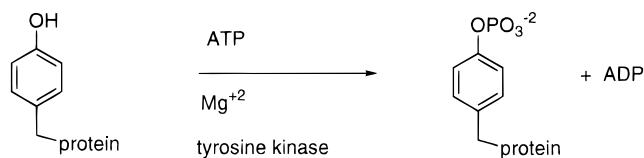


Figure 1. Protein tyrosine kinase-catalyzed reaction.

studied in recent years.<sup>2</sup> There is a major pharmaceutical effort to develop specific inhibitors of these enzymes as drugs.<sup>3</sup>

The amino acid sequences and three-dimensional structures of protein serine/threonine-specific kinases and tyrosine-specific kinases are highly conserved.<sup>4</sup> Many of the amino acids that

\* To whom correspondence should be addressed: tel, (212) 327-7241; fax, (212) 327-7243; e-mail, cole@rockvax.rockefeller.edu.

(1) (a) Hunter, T. *Cell* **1995**, *80*, 225–236. (b) Shokat, K. M. *Chem. Biol.* **1995**, *2*, 509–514.

(2) (a) Cheng, H. J.; Flanagan, J. G. *Cell* **1994**, *79*, 157–168. (b) Banker, N.; Evers, B. M.; Hellmich, M. R.; Townsend, C. M. *Surg. Oncol.* **1996**, *5*, 201–210. (c) Creedon, D. J.; Tansey, M. G.; Baloh, R. H.; Osborne, P. A.; Lampe, P. A.; Fahrner, T. J.; Heuckeroth, R. O.; Millbrandt, J.; Johnson, E. M. *Proc. Natl. Acad. Sci. U.S.A.* **1997**, *94*, 7018–7023. (d) White, M. F.; Kahn, C. R. *J. Biol. Chem.* **1994**, *269*, 1–4. (e) Heyeck, S. D.; Wilcox, H. M.; Bunnell, S. C.; Berg, L. J. *J. Biol. Chem.* **1997**, *272*, 25401–25408.

(3) (a) Levitzki, A.; Gazit, A. *Science* **1995**, *267*, 1782–1788. (b) Mohammadi, M.; McMahon, G.; Sun, L.; Tang, C.; Hirth, P.; Yeh, B. K.; Hubbard, S. R.; Schlessinger, J. *Science* **1997**, *276*, 955–960.

(4) (a) Madhusudan; Trafny, E. A.; Xuong, N.-H.; Adams, J. A.; Ten Eyck, L. F.; Taylor, S. S.; Sowadski, J. M. *Protein Sci.* **1994**, *3*, 176–187. (b) Johnson, L. N.; Noble, M. E. M.; Owen, D. J. *Cell* **1996**, *85*, 149–158. (c) Xu, W.; Harrison, S. C.; Eck, M. J. *Nature* **1997**, *385*, 595–601. (d) Sicheri, F.; Moarefi, I.; Kuriyan, J. *Nature* **1997**, *385*, 602–608.

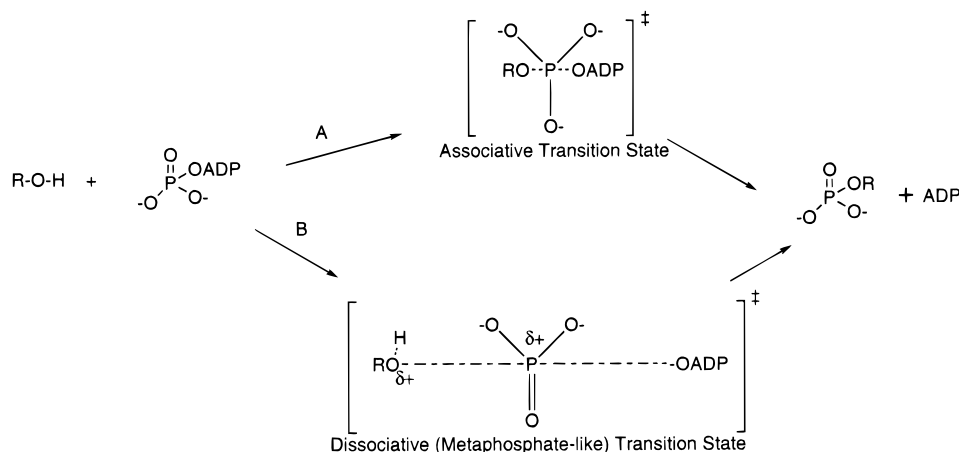


**Figure 2.** Associative vs dissociative transition states for phosphoryl transfer. ROH is the nucleophile (tyrosine phenol in this work) attacking the  $\gamma$ -phosphoryl group of ATP, and ADP is the leaving group. Associative transition state (path A) in this work is defined as more than 50% bond formation between the nucleophilic oxygen and the phosphorus, which occurs with at least 50% leaving group residual bond formation present.<sup>5</sup> Dissociative transition state (path B) in this work is defined as less than 50% bond formation between the nucleophile and the phosphorus, which occurs before the leaving group–phosphorus bond is at least 50% broken.

make up the catalytic active site of protein kinases are identical within the superfamily. The nature of the transition state in protein kinase reactions, which fundamentally sets the boundaries for the biologically topical issues of regulation and substrate selection, has not yet been fully elucidated.

In general, the mechanisms of nonenzymatic phosphoryl transfer reactions are fairly well-understood.<sup>5</sup> Nonenzymatic phosphate monoester reactions follow dissociative mechanisms where the bond between phosphorus and the leaving group is largely broken in the transition state and the bond between the nucleophile and phosphorus is minimally formed in the transition state (Figure 2). It has been argued that enzymes can render phosphoryl transfer transition states more associative by surrounding the attacked phosphate with positively charged groups, making the phosphate a better electrophile by neutralizing its negative charge.<sup>6</sup> Justification for this analysis has in part been based on nonenzymatic phosphate triester reactions that show associative character.<sup>7</sup> A judiciously positioned active site base revealed by crystallographic studies of protein kinases has been suggested to make the hydroxyl nucleophile more reactive in enzymatic reactions, facilitating an associative phosphoryl transfer reaction mechanism for protein kinases.<sup>8</sup> However, a long reaction coordinate distance of 5.2 Å between the entering hydroxy nucleophile and the ATP  $\gamma$ -phosphoryl group in the serine/threonine protein kinase A active site has been taken as evidence for a dissociative mechanism.<sup>6c</sup>

Linear free-energy relationships have proven useful in clarifying reaction mechanisms in physical organic chemistry.<sup>9</sup> The Brønsted nucleophile coefficient ( $\beta_{\text{nuc}}$ ), a measure of the role of the nucleophile in the transition state, has been determined

for a wide variety of nonenzymatic phosphate monoester phosphoryl transfer reactions and has been shown to be small (0–0.3) for this class of reactions.<sup>10</sup> A small  $\beta_{\text{nuc}}$  is expected for a dissociative mechanism since there is little bond formation between the nucleophile and phosphorus in the transition state. In contrast, nonenzymatic phosphate triester reactions typically exhibit large  $\beta_{\text{nuc}}$  values (0.5–0.9) more consistent with an associative mechanism.<sup>7</sup>

Linear free-energy relationships are often more difficult to obtain in enzyme systems because of the typically strict requirements for substrate active site binding. Thus, obtaining a series of homologous substrates that differ in nucleophile  $\text{p}K_{\text{a}}$  but bind to the enzyme active site with similar affinity and orientation is often not possible. In principle, a protein tyrosine kinase reaction is amenable to such studies because the substrate tyrosine aromatic ring can be substituted in ways that might not be too disruptive to binding or catalysis. Recently, using a series of fluorotyrosine-containing peptides as substrates, a  $\beta_{\text{nuc}}$  for  $k_{\text{cat}}$  and  $k_{\text{cat}}/K_{\text{m}}$  of 0–0.1 was reported for protein tyrosine kinase Csk-catalyzed phosphorylation.<sup>11</sup> By comparing the reaction rates at pH 7.4 and pH 6.6 for several of the analogues, it was suggested that the neutral phenol rather than the phenoxide anion was the preferred nucleophile for the enzyme reaction.<sup>11</sup>

Measurements of the  $\beta_{\text{leaving group}}$  can provide complementary information about the transition states of phosphoryl transfer reactions. Large negative  $\beta_{\text{leaving group}}$  values (ca. –1) are usually observed with nonenzymatic phosphate monoester phosphoryl transfer reactions at neutral pH, indicating that the transition state shows significant negative charge buildup on the leaving group and therefore a high degree of bond cleavage between phosphorus and the leaving group. Under acidic conditions (e.g., pH 4), a more modest  $\beta_{\text{leaving group}}$  value (–0.3) is associated with hydrolyses of phosphate monoesters because proton transfer to the departing oxygen atom is a critical feature of the transition state.<sup>12</sup>

In an effort to improve understanding of protein kinase catalysis, in this study we report the results of a detailed kinetic

(5) (a) Admiraal, S. J.; Herschlag, D. *Chem. Biol.* **1995**, *2*, 729–739. (b) Maegley, K. A.; Admiraal, S. J.; Herschlag, D. *Proc. Natl. Acad. Sci. U.S.A.* **1996**, *93*, 8160–8166.

(6) (a) Mildvan, A. S.; Fry, D. C. *Adv. Enzymol. Relat. Areas Mol. Biol.* **1987**, *59*, 241–313. (b) Schlichting, I.; Reinstein, J. *Biochemistry* **1997**, *36*, 9290–9296. (c) Granot, J.; Mildvan, A. S.; Bramson, H. N.; Kaiser, E. T. *Biochemistry* **1980**, *19*, 3537–3543.

(7) (a) Khan, S. A.; Kirby, A. J. *J. Chem. Soc. B*, **1970**, 1172–1182. (b) Epstein, J.; Plapinger, R. E.; Michel, H. O.; Cable, J. R.; Stephani, R. A.; Billington, C. A.; West, G. R. *J. Am. Chem. Soc.* **1964**, *86*, 3075–3084.

(8) (a) Bossemeyer, D.; Engh, R. A.; Kinzel, V.; Pongstingl, H.; Huber, R. *EMBO J.* **1993**, *12*, 849–859. (b) Zheng, J.; Knighton, D. R.; Ten Eyck, L. F.; Karlsson, R.; Xuong, N.-H.; Taylor, S. S.; Sowadski, J. M. *Biochemistry* **1993**, *32*, 2154–2161.

(9) Jencks, W. P. *Catalysis in Chemistry and Enzymology*; McGraw-Hill: New York, 1969.

(10) (a) Kirby, A. J.; Varvoglis, A. G. *J. Chem. Soc. B* **1968**, 135–141. (b) Herschlag, D.; Jencks, W. P. *J. Am. Chem. Soc.* **1987**, *109*, 4665–4674.

(11) Kim, K.; Cole, P. A. *J. Am. Chem. Soc.* **1997**, *119*, 11096–11097.

(12) Kirby, A. J.; Varvoglis, A. G. *J. Am. Chem. Soc.* **1967**, *89*, 415–423.

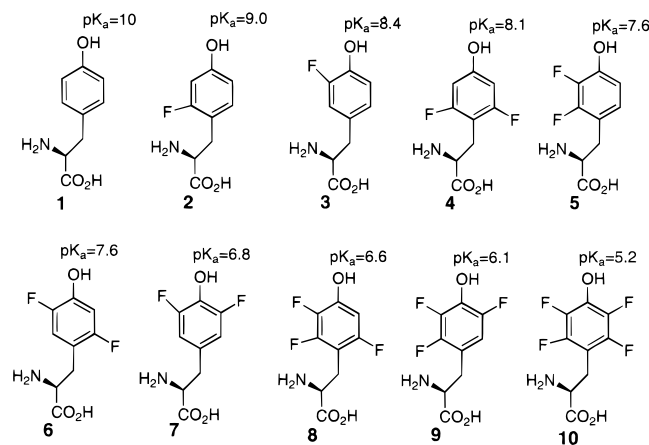


**Figure 3.** Fluorotyrosine analogues used in this work.

investigation on protein tyrosine kinase-catalyzed phosphoryl transfer reactions to and from fluorotyrosine peptide substrates. These studies further support the proposal of a dissociative reaction mechanism with the neutral phenol acting as the preferred substrate nucleophile.

## Results and Discussion

### Synthesis of Fluorotyrosine Amino Acids and Peptides.

Standard total chemical synthesis of the nine fluorotyrosine amino acids (Figure 3) used in these investigations would be laborious. For example, the known amino acid tetrafluorotyrosine (**10**) is obtained from hexafluorobenzene in five steps to afford racemic amino acid.<sup>13</sup> Syntheses of several of the other di- and trifluorotyrosines could be expected to be at least as difficult by standard routes. Separation and characterization of the individual enantiomers is also a tedious process. Fortunately, the enzyme tyrosine phenol-lyase has been shown to be a highly efficient and rather general catalyst for the incorporation of substituted phenols into L-tyrosine derivatives.<sup>14</sup> Gram quantities of the fluorotyrosine amino acids using the recombinant enzyme tyrosine phenol-lyase were prepared from the phenols in the presence of pyruvate and  $\text{NH}_3$ . To generate tetrafluorotyrosine (**10**), extended reaction times and greater quantities of tyrosine phenol-lyase enzyme were required. The reduced processing efficiency of tetrafluorophenol may be due to a combination of increased steric bulk and/or a decreased ability to stabilize positive charge in the aryl group in the transition state.

The unprotected fluorotyrosine amino acids (**X**, Figure 3) were reacted with Fmoc-O-succinimidyl carbonate and the Fmoc amino acids were used to generate the peptides  $\text{NH}_2\text{-Glu-Asp-Asn-Glu-X-Thr-Ala-CO}_2\text{H}$  by automated solid-phase peptide synthesis using a 0.1–0.25 mmol scale. Peptides were obtained in approximately 50% yield after purification.

**Phosphorylation vs pH.** Given the preliminary pH rate studies presented for the various fluorotyrosine peptides reported earlier,<sup>11</sup> it was important to try to fully establish the true correlation between the  $\text{pK}_a$  of the phenol and the kinetics of the kinase reaction in a more extensive analysis. In principle, the titration of acid/base groups versus pH should reflect the free substrate and enzyme form when analyzing  $\log(k_{\text{cat}}/K_m)$  vs pH whereas they should reflect the bound enzyme/substrate

complex when plotting  $\log(k_{\text{cat}})$  vs pH.<sup>15a</sup> Four of the fluorotyrosine peptides and the unfluorinated tyrosine-containing peptide were assayed ( $k_{\text{cat}}/K_m$  measurements) with Csk covering the pH range 6–8.6 (Figure 4). It proved impossible to obtain complete data sets for the corresponding  $k_{\text{cat}}$  plots because the  $K_m$  values in some cases were too high to be accurately measured.

A plot of the  $\log k_{\text{cat}}/K_m$  vs pH for the unfluorinated tyrosine-containing peptide showed an increase in rate from pH 6 to pH 7 and then reached a plateau (Figure 4A). This behavior fits reasonably well to a model with a single ionizable group (corresponding to  $\text{pK}_1$ ) with  $\text{pK}_a$  near 7 that facilitates phosphoryl transfer in its deprotonated form. Given this  $\text{pK}_a$  value, it is unlikely that the proposed ionizable group comes from the peptide substrate since in free solution EDNEYTA lacks such a  $\text{pK}_a$ . At this time, it is unclear whether this proposed ionizable group is involved in substrate binding or phosphoryl transfer, although the former is favored because of the lack of a pH rate effect in this region for Csk-catalyzed phosphorylation of the substrate poly(glu,tyr).

Kinase kinetic analysis of the substrate fluorotyrosine peptide derivatives showed evidence of a similar titratable group ( $\text{pK}_1$ ) to that found with the unfluorinated peptide, although with a slightly higher  $\text{pK}_a$  (7.5–8) (Figure 4B–E). However, instead of a plateau at the higher pH, the  $k_{\text{cat}}/K_m$  decreased above pH 8 in all cases, suggestive of an additional group ( $\text{pK}_2$ ) leading to decreased kinase activity in its deprotonated form. The theoretical fit of the data in Figure 4B–E revealed that the value of  $\text{pK}_2$  was lower than the value of  $\text{pK}_1$  for these substrates. The  $\text{pK}_a$  values of the fluorotyrosine phenols measured spectrophotometrically agree nicely with those extrapolated from the kinetic analyses ( $\text{pK}_2$ ) in plots of  $\log(k_{\text{cat}}/K_m)$  vs pH (Table 1). These results provide convincing evidence that the neutral phenol of the tyrosine and fluorotyrosine derivatives rather than the phenoxide anion is the reactive nucleophile in the enzymatic reaction. The more chemically reactive phenoxide anion species in contrast appears inactive in the enzymatic phosphoryl transfer reactions.

Deprotonation of the tyrosine hydroxyl is a necessary feature of phosphoryl transfer to the phenol along the reaction coordinate. Therefore, it is important to consider the circumstances that could account for the neutral phenol behaving as a ‘more reactive’ nucleophile than the free phenoxide anion in the enzyme reaction. In an associative mechanism, with significant participation of the nucleophile in the transition state, a typical  $\beta_{\text{nuc}}$  value is 0.6.<sup>7</sup> Since the  $\text{pK}_a$  values of the phenol and phenoxide anions differ by  $\sim 17$  units,<sup>15b</sup> the phenoxide anion is expected to react approximately  $10^{10}$ -fold faster than the neutral phenol assuming identical orientation and binding behavior. The transition state energy barrier for phenoxide ion nucleophilic attack would thus be approximately 14 kcal/mol lower as compared to the neutral phenol. In order for the phenoxide ion to be a less successful nucleophile in the associative mechanism (if the  $\beta_{\text{nuc}} = 0.6$ ), disrupted binding forces costing more than 14 kcal/mol energy would apparently be required. While the loss of a hydrogen bond and/or electrostatic repulsion in the neutral versus anionic species could contribute in part to such a binding disruption, it would be difficult to account for such a large energy change by these factors alone.

However, in a dissociative mechanism where a typical value of  $\beta_{\text{nuc}}$  is 0.1, the phenoxide anion would only be expected to

(13) Filler, R.; Ayyangar, N. R.; Gustowski, W.; Kang, H. H. *J. Org. Chem.* **1969**, *34*, 534–538.

(14) (a) Hebel, D.; Furlano, D. C.; Phillips, R. S.; Koushik, S.; Creveling, C. R.; Kirk, K. L. *Bioorg. Med. Chem. Lett.* **1992**, *2*, 41–44. (b) Nagasawa, T.; Utagawa, T.; Goto, J.; Kim C.-J.; Tani, Y.; Kumagai, H.; Yamada, H. *Eur. J. Biochem.* **1981**, *117*, 33–40.

(15) (a) Dixon, M.; Webb, E. C. *Enzymes*; Academic Press: New York, 1964. (b) Wu, C. Y.; Arnett, E. M. *J. Am. Chem. Soc.* **1960**, *82*, 5660–5665.

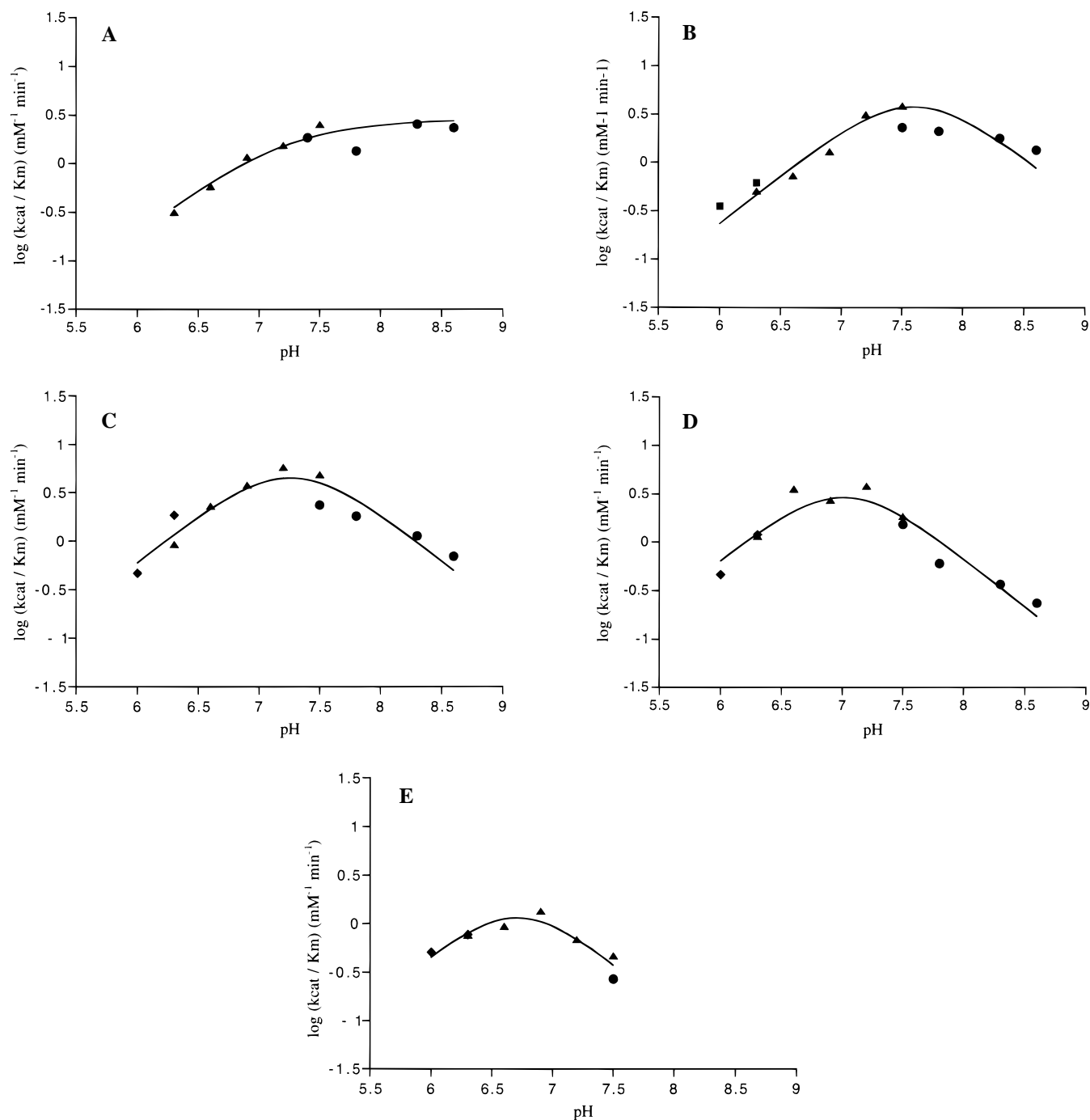


**Figure 4.** Profiles of  $\log(k_{\text{cat}}/K_m)$  vs pH for peptides containing fluorotyrosine analogues **1**, **6**, and **8–10** (A–E, respectively). Symbols: Diamonds, Bis-Tris-HCl buffer; triangles, Mops-Na buffer; circles, Tris-HCl buffer. See Experimental Section for other details. In this work, the  $pK_a$  corresponding to the acidic limb of the profiles is defined as  $pK_1$ , and that corresponding to the basic limb is defined as  $pK_2$ . The calculated acidity constants  $\pm$  standard error for each of the plots are as follows: A,  $pK_1 = 7.0 \pm 0.1$ ; B,  $pK_1 = 7.9 \pm 0.1$ ,  $pK_2 = 7.3 \pm 0.1$ ; C,  $pK_1 = 7.6 \pm 0.2$ ;  $pK_2 = 6.9 \pm 0.3$ ; D,  $pK_1 = 7.7 \pm 0.3$ ;  $pK_2 = 6.3 \pm 0.2$ ; E,  $pK_1 = 7.8 \pm 0.8$ ;  $pK_2 = 5.6 \pm 0.8$ .

react about 50-fold faster as compared to the neutral phenol, corresponding to approximately 2 kcal/mol lowering of the transition state energy barrier. Under these conditions, the loss of a hydrogen bond and/or electrostatic repulsion could dominate the expected rate effects due to loss of nucleophilicity. Thus the combination of a low  $\beta_{\text{nuc}}$  and a requirement for a neutral phenol are persuasive evidence for a dissociative mechanism.

What specific factors could be responsible for the lack of reaction of the negatively charged nucleophile in the Csk kinase

**Table 1.** Substrate Phenolic Spectrophotometric  $pK_a$  Values Correlated with Enzyme (Forward Reaction) Kinetic  $pK_a$  Values<sup>a</sup>

tyrosine analog	spectrophotometric $pK_a$	kinetic $pK_a$
<b>1</b>	10	>8
<b>6</b>	7.6	$7.3 \pm 0.1$
<b>8</b>	6.6	$6.9 \pm 0.3$
<b>9</b>	6.1	$6.3 \pm 0.2$
<b>10</b>	5.2	$5.6 \pm 0.8$

<sup>a</sup> The kinetic  $pK_a$  values are defined as the  $pK_a$  values (the basic limbs) from Figure 4. For details of the measurements, see the Experimental Section.

reaction?<sup>16</sup> Possibilities include repulsion by the negatively charged phosphate oxygens<sup>17</sup> and/or the highly conserved active site aspartate carboxylate anion (asp-314 in Csk).<sup>4</sup> There are several reports discussing the potential repulsion of negatively charged nucleophiles by the phosphate oxygens in phosphate monoesters.<sup>17,18</sup> Approximately 2 kcal/mol electrostatic repulsion energy between anionic nucleophiles and phosphate monoesters has been estimated from model systems.<sup>17</sup> In combination with the predicted loss of hydrogen bonding and gain of electrostatic repulsion between the asp-314 carboxylate and the phenoxide anion, it is reasonable to rationalize the 4–5 kcal/mol energy loss required to explain the decreased efficiency of the phenoxide anion as nucleophile in the enzymatic reaction.

Analysis of the  $k_{\text{cat}}$  vs pH for enzymes can provide information about the  $\text{p}K_{\text{a}}$  values of groups in the bound complex. Because of the already low affinity of the peptide substrates used in this work for Csk, accurate  $k_{\text{cat}}$  values could not be obtained for the fluorotyrosine analogues at some of the pHs. However, from the available data (not shown), it could be estimated that the  $k_{\text{cat}}$  values vs pH showed similar behavior to the  $k_{\text{cat}}/K_{\text{m}}$  vs pH. The  $\text{p}K_{\text{a}}$  of the substrate tyrosine is probably  $\pm 2$  units in the enzyme active sites compared to its value in free solution. Theoretically, altering the  $\text{p}K_{\text{a}}$  of the nucleophile would serve little purpose in facilitating a dissociative mechanism.

**$\beta_{\text{leaving group}}$  for the Reverse Reaction.** In principle, obtaining the  $\beta_{\text{leaving group}}$  for a protein tyrosine kinase reaction would involve studying ATP analogues with a range of  $\text{p}K_{\text{a}}$  values for the  $\beta$ -phosphate of the leaving ADP moiety. It is unlikely that the necessary modifications would be compatible with enzymatic catalysis because they would significantly alter the steric and electronic properties of the ADP molecule. In contrast, a more realistic goal appeared to be evaluating the  $\beta_{\text{leaving group}}$  for the reverse kinase (ATP synthesis) reaction. The equilibrium constant was expected to be approximately 10 for tyrosine phosphorylation in the forward direction at neutral pH.<sup>19</sup> Kinetic analysis of the reverse reaction with ADP as the nucleophile and the tyrosine phenol as the leaving group therefore seemed plausible since the requisite substituted tyrosine derivatives were already accessible.

The necessary phosphopeptides were obtained by enzymatic phosphorylation of the fluorotyrosine-containing peptides using recombinant Csk. The phosphorylated peptides were very well separated from the unphosphorylated forms by reverse-phase HPLC using a standard water:acetonitrile gradient (see Figure 5), and electrospray ionization mass spectrometry confirmed their identity. These phosphopeptides were stable in frozen solution at  $-80$  °C for extended periods.

Csk enzymatic assay of the phosphopeptides in the ATP synthesis direction was carried out. The reverse kinase reactions proved to be too slow to be accurately monitored with the

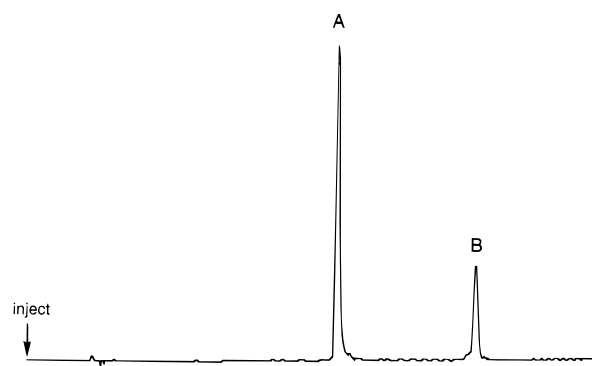


**Figure 5.** HPLC trace of phosphopeptide and peptide containing fluorotyrosine derivative (**8**). HPLC conditions were as follows: C-18 analytical column, water:acetonitrile gradient (0.05% trifluoroacetic acid); 0–10 min, 0–10% acetonitrile; 10–20 min, 10–15% acetonitrile; 20–30 min, 15–25% acetonitrile. UV monitoring at 214 nm was carried out. Peak A represents phosphopeptide (retention time, 16 min) and peak B corresponds to unphosphorylated peptide (retention time, 24 min).

standard hexokinase/glucose-6-phosphate dehydrogenase spectrophotometric assay<sup>20</sup> due to high background. Instead, an HPLC assay with direct monitoring of conversion to the dephosphorylated peptide was employed. Background hydrolysis rates of the phosphopeptides under these conditions (presumed to be related to trace quantities of contaminating phosphatases) were measured by omitting ADP from the reaction mixtures and for six of the peptides shown to be less than 15% of the total rates. In the four cases where the background rate was significant (40–70% of the total rate, see Experimental Section), it was found to be reproducible and was subtracted from the total rate to obtain the true reverse kinase rates. Product formation was shown to be linear with time for at least 1 h and with enzyme concentration in the range of 1–10  $\mu\text{M}$ . Enzyme activity versus phosphopeptide concentration was found to be linear in the 1–4 mM range for all peptides examined so that  $k_{\text{cat}}/K_{\text{m}}$  (but not  $k_{\text{cat}}$ ) could be readily measured under these conditions. Studies in the forward kinase direction and previous inhibitor analyses indicate that the fluorotyrosines bind with similar affinity (over a 3-fold range)<sup>11,16</sup> so the absence of direct  $K_{\text{m}}$  measurements for the reverse reaction was not considered a liability. The rate ( $k_{\text{cat}}/K_{\text{m}}$ ) for the standard tyrosine (**1**)-containing peptide allows an estimate of the equilibrium constant ( $[\text{phosphopeptide}][\text{ADP}]/[\text{peptide}][\text{ATP}]$ ) of approximately 23 (at pH 7.4, in the forward kinase direction) assuming the ADP  $K_{\text{m}}$  is approximately 5-fold greater than the  $K_{\text{m}}$  for ATP and the mechanism is ‘rapid equilibrium random’ with Mg.<sup>21</sup> This is in fairly good agreement with the value of 10 measured with a different peptide substrate with the Src enzyme.<sup>19</sup>

Analysis of the  $\log(k_{\text{cat}}/K_{\text{m}})$  vs leaving group  $\text{p}K_{\text{a}}$  is shown in Figure 6. The slope which equals the  $\beta_{\text{leaving group}}$  was calculated by linear regression to be  $-0.33 \pm 0.06$ . This value is considerably less negative than that commonly observed for phosphate monoester phosphoryl transfer reactions<sup>5a</sup> and would even be low for diesters (typically  $-0.9$  to  $-1.1$ )<sup>18</sup> and triesters (typically  $-0.4$  to  $-1$ ).<sup>7a</sup> One possibility for this small effect is that the more highly fluorinated compounds do not bind as well to the enzyme, which could offset more marked  $k_{\text{cat}}$  rate effects. Evidence against this possibility comes from studies in the forward direction where the  $K_{\text{m}}$  values (which are likely

(16) The simple possibility that the phenoxide anion is unable to bind to Csk is unlikely. Titrating the peptide containing tetrafluorotyrosine (1–16 mM) as an inhibitor (at pH 7.4 in which approximately 99% exists in the phenoxide anionic form) of Csk phosphorylation [fixed substrate concentration of EDNEYTA (4 mM)] showed that it was a linear inhibitor with a  $K_{\text{i}}$  of  $4.6 \pm 0.5$  mM assuming a competitive inhibition model. This  $K_{\text{i}}$  is in good agreement with the  $K_{\text{m}}$  of EDNEXTA peptides<sup>11</sup> at this pH as well as with the  $K_{\text{i}}$  of EDNEFTA (demonstrated to be a linear competitive inhibitor versus poly(glu, tyr) with a  $K_{\text{i}}$  of  $4.9 \pm 0.7$  mM<sup>21</sup> and the deduced  $K_{\text{i}}$  values of EDNEYTA and EDNEXTA ( $X = 9$ ) versus the substrate poly(glu, tyr).<sup>24</sup>

(17) Herschlag, D.; Jencks, W. P. *J. Am. Chem. Soc.* **1989**, *111*, 7587–7596.

(18) Kirby, A. J.; Younas, M. *J. Chem. Soc. B.* **1970**, 1165–1172.

(19) Boerner, R. J.; Barker, S. C.; Knight, W. B. *Biochemistry* **1995**, *34*, 16419–16423.

(20) Oliver, I. T. *J. Biol. Chem.* **1955**, *61*, 116–122.

(21) Grace, M. R.; Walsh, C. T.; Cole, P. A. *Biochemistry* **1997**, *36*, 1874–1881.

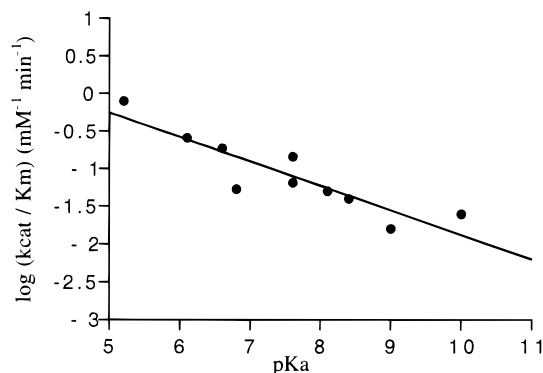


**Figure 6.** Brønsted plot of the  $\log(k_{\text{cat}}/K_{\text{m}})$  versus the tyrosine phenol  $\text{p}K_{\text{a}}$  values for the reverse Csk tyrosine kinase reactions with substrates ADP and phosphopeptides (with tyrosine derivatives **1–10**). See the Experimental Section for details. The  $\beta_{\text{leaving group}}$  (slope  $\pm$  standard error) was calculated using linear regression and found to be  $-0.33 \pm 0.06$ . Equal to  $K_{\text{d}}$  values) for the various peptides were shown to be similar (within a 3-fold range) regardless of the number of fluorines in the peptides. A second possibility is that the reaction is not limited by chemistry. This possibility seems unlikely since the reactions in the forward direction (which are faster) are very likely to be limited by chemistry, and ATP and peptide likely have fast off rates.<sup>11,21</sup> A third possible explanation is that the reverse kinase reaction is highly associative. This is very unlikely given the law of microscopic reversibility based on the fact that the forward direction is likely dissociative for reasons discussed above.

The most likely explanation for the low  $\beta_{\text{leaving group}}$  is that the transition state involves protonation of the leaving group by an active site acid group, which would attenuate the buildup of effective negative charge on the departing oxygen.<sup>22</sup> Such an effect has been observed in the hydrolysis of phosphate monoesters at pH 4. In fact, a nearly identical  $\beta_{\text{leaving group}}$  value of  $-0.27$  was observed in this nonenzymatic reaction model system.<sup>12</sup> The facilitation of leaving group departure would appear to be a key feature of dissociative transition states, and the use of an active site acid to protonate the leaving group oxygen would accomplish this objective. As mentioned above, the active nucleophilic species in the forward kinase direction appears to be the neutral phenol. Since the law of microscopic reversibility requires that the protonation state of the phenol in the transition state be identical in both directions, a large negative  $\beta_{\text{leaving group}}$  effect (e.g.,  $-1$ ) would be incompatible with the mechanistic model based on studies of the forward kinase direction.

While the identity of the active site acid group is not known with certainty, it seems most reasonable to suggest that in Csk it is Asp-314. A recent crystal structure of the insulin receptor protein tyrosine kinase revealed that this conserved aspartate hydrogen bonds to the nucleophilic hydroxy group.<sup>23</sup> Moreover, mutation of this conserved aspartate in Csk<sup>21,24</sup> and the corresponding residue in protein kinase A<sup>25,26</sup> have been shown to be associated with a reduction in  $k_{\text{cat}}$  of approximately  $10^4$  on the chemical step for both. In the forward direction, the aspartate is expected to direct and orient the hydroxyl group toward the  $\gamma$ -phosphate. Its role as a “catalytic base” if any would be expected to take place well after the tyrosine-phosphate bond is largely formed.

(22) Williams, A. *Adv. Phys. Org. Chem.* **1992**, *27*, 1–55.

(23) Hubbard, S. R. *EMBO J.* **1997**, *16*, 5572–5581.

(24) Cole, P. A.; Grace, M. R.; Phillips, R. S.; Burn, P.; Walsh, C. T. *J. Biol. Chem.* **1995**, *270*, 22105–22108.

(25) Gibbs, C. S.; Zoller, M. J. *Biochemistry* **1991**, *30*, 8923–8931.

(26) Zhou, J.; Adams, J. A. *Biochemistry* **1997**, *36*, 2977–2984.

**Dissociative Mechanism for Protein Kinases.** Through the use of  $\beta_{\text{nuc}}$  measurements, pH rate analyses, and  $\beta_{\text{leaving group}}$  studies, a picture emerges of the protein kinase mechanism in which the transition state of the reaction is dissociative. In such a mechanism, there is relatively little bond formation between the attacking nucleophile (serine or tyrosine) and the phosphorus prior to departure of the leaving group (ADP). Although it is very hard to prove enzymatic mechanisms with absolute certainty, there is no existing evidence that contradicts this model. Short reaction coordinate distances between the entering serine oxygen and the  $\gamma$ -phosphorus of enzyme-bound ATP of 2.7–3.1 Å were obtained by X-ray crystallography studies on protein kinase A<sup>4a,8</sup> while a longer reaction coordinate distance (5.2 Å) was obtained by NMR.<sup>6c</sup> A recent X-ray crystallographic analysis of insulin receptor tyrosine kinase showed a 5 Å reaction coordinate distance in a ternary complex.<sup>23</sup> All of these studies have required the use of unreactive substrate analogues that make their reliability uncertain. Although a large  $k_{\text{cat}}$  thio effect for a Csk reaction was initially taken as evidence of an associative mechanism,<sup>24</sup> more detailed studies with various thiophilic metal ions have argued that the thio effect is largely a matter of impaired metal coordination rather than electronegativity changes due to sulfur.<sup>21</sup> Furthermore, <sup>18</sup>O-isotope effects, while small and sometimes difficult to interpret, have generally supported the concept that other phosphate monoester enzymatic reactions are dissociative.<sup>27</sup>

From a theoretical standpoint, a cogent argument has been advanced that if the enzyme were to render the transition state more associative than the transition state of the nonenzymatic reaction, it would have to supply greater stabilization than to stabilize a dissociative mechanism.<sup>5</sup> Perhaps the most unsettling aspect of dissociative enzymatic mechanisms for protein kinases is that it is not so obvious how precise product formation could be achieved. It is true that some protein kinases have low ATPase activity, but the presumption is that there must be rigid geometric constraints for the binding of the nucleophile before leaving group departure is activated. Many of the active site residues would have key orientational roles in this model. In protein kinases, the key activating residues would be those that effect rupture of the  $\gamma$ -phosphate– $\beta$ -phosphate bridging oxygen bond. While there is no hard information on this point, the possible key participants would be one of the divalent ions and/or a conserved active site lysine.<sup>4</sup>

**Implications of a Dissociative Mechanism.** There is a major effort in the cell signal transduction community in characterizing protein kinases in order to understand the basis of substrate selectivity and to discern how the enzymes are regulated.<sup>1,2,4</sup> Pharmacologists are interested in designing specific inhibitors of these enzymes that might have therapeutic value for a wide range of diseases.<sup>3</sup> The predicted dissociative transition state distance between the entering nucleophilic hydroxyl oxygen and the departing ADP oxygen is on the order of 1–2 Å larger than in an associative transition state.<sup>28</sup> To model the role of amino acids in the active site that would stabilize such a transition state and dictate substrate selection, it is helpful to have knowledge of the fundamental strategy the enzyme uses in effecting catalysis. Likewise, in describing the “inactive” versus “active” structures of the enzymes, a major goal of structural biologists, it would seem essential to define the electronic requirements of the “active” state. Successful transition state analogue inhibitor design would appear to require the develop-

(27) Jones, J. P.; Weiss, P. M.; Cleland, W. W. *Biochemistry* **1991**, *30*, 3634–3639.

(28) Mildvan, A. S. *Proteins: Struct. Funct. Genet.* **1997**, *29*, 401–416.

ment of a compound that could fill the relatively larger molecular space occupied by a dissociative transition state.

## Experimental Section

**Expression and Purification of Tyrosine Phenol-Lyase.** The protocol is based on the method of Phillips and colleagues.<sup>29</sup> Single colonies of the SVS370 *Escherichia coli* strain carrying the DNA plasmid pTZTPL were used to inoculate 3 × 1 L of LB medium containing ampicillin (100 μg/mL), and the cultures were grown at 37 °C for 20 h in a shaker/incubator. Cells were harvested by centrifugation (30 min, 10000g) affording 20 g, snap frozen, and stored at -80 °C until needed. The thawed cells were suspended in 80 mL of standard buffer (0.1 M potassium phosphate, pH 7.0, 0.1 mM pyridoxal phosphate, 1 mM EDTA, and 5 mM β-mercaptoethanol) and lysed by passage through a French pressure cell (600 psi). The resultant suspension was centrifuged for 30 min at 25000g at 4 °C, and the recovered supernatant was treated with 2% w/v protamine sulfate (12 mL) by dropwise addition at room temperature. The resultant cloudy solution was centrifuged for 30 min at 25000g at 4 °C, and the clear yellow supernatant was brought to 60% saturation with the addition of solid (NH<sub>4</sub>)<sub>2</sub>SO<sub>4</sub> at 4 °C. The resultant suspension was centrifuged for 30 min at 25000g, and the pellet was dissolved in standard buffer and dialyzed against standard buffer, 25% saturated with (NH<sub>4</sub>)<sub>2</sub>SO<sub>4</sub> overnight at 4 °C. The protein solution was loaded onto the previously equilibrated octyl-Sepharose column (11 cm × 2 cm) with the standard buffer 25% saturated with (NH<sub>4</sub>)<sub>2</sub>SO<sub>4</sub> at 1 mL/min. After continuing to elute with standard buffer 25% saturated with (NH<sub>4</sub>)<sub>2</sub>SO<sub>4</sub>, early fractions (about 150 mL) containing tyrosine phenol-lyase were combined, precipitated with 75% saturating (NH<sub>4</sub>)<sub>2</sub>SO<sub>4</sub>, resuspended, and dialyzed against standard buffer to afford 80 mL of tyrosine phenol-lyase solution at a concentration of 5 mg/mL protein. A 10% SDS-PAGE stained with Coomassie showed that tyrosine phenol-lyase was approximately 70% pure. Lyase activity assay (lactate dehydrogenase coupled assay with NADH spectrophotometric monitoring at 340 nm)<sup>29</sup> with tyrosine as substrate demonstrated that there was a total of 1200 units of lyase activity in the final preparation, which was stored at -80 °C in 1-mL aliquots.

**Synthesis of Fluorotyrosine Analogues (2–10).** For the standard reaction, an aqueous solution (1 L) of fluorophenol (10 mM), pyruvic acid (60 mM), pyridoxal-5'-phosphate (10 mg/L), ammonium acetate (30 mM), β-mercaptoethanol (5 mM), and 30 units of tyrosine phenol-lyase (TPL) was adjusted to pH 8 with dilute NH<sub>4</sub>OH and stored in the dark at room temperature for 3–4 days.<sup>14</sup> In the case of tetrafluorophenol, 150 units of tyrosine phenol-lyase was added, and the reaction was allowed to proceed for 2–3 weeks at room temperature. The mixture was then acidified with acetic acid (to achieve pH 3) and filtered through a pad of Celite. The filtrate was extracted with 500 mL of ethyl acetate to remove unreacted fluorophenol. A prewashed (6 N HCl, 6 N NaOH, water) cation exchange column (20 g of Dowex-50W) was loaded with the reaction mixture, and the column was washed with 5 column volumes of water followed by elution with 10% NH<sub>4</sub>OH (aqueous). Fractions that gave a positive ninhydrin reaction were combined and lyophilized to give a white solid, which was shown to be pure fluorotyrosine analogue (0.5–2 g of product). Each analogue was characterized using <sup>1</sup>H NMR, <sup>19</sup>F NMR, and HRMS with the data shown below:

**2-Fluorotyrosine (2).** <sup>1</sup>H NMR (D<sub>2</sub>O); δ 7.00 (brs, 1 H), 6.54 (brs, 2 H), 3.99 (m, 1 H), 3.90 (m, 1 H), 2.74 (m, 1 H). <sup>19</sup>F NMR (D<sub>2</sub>O); δ -116 (t, *J* = 10 Hz, 1 F). HRMS calcd. for C<sub>9</sub>H<sub>10</sub>NO<sub>3</sub>F (MH)<sup>+</sup>, 200.0723; found, 200.0723.

**3-Fluorotyrosine (3).** <sup>1</sup>H NMR (D<sub>2</sub>O); δ 7.09 (d, *J* = 11.7 Hz, 1 H), 6.98 (m, 2 H), 3.94 (dd, *J* = 8.0, 5.1 Hz, 1 H), 3.21 (dd, *J* = 14, 5.1 Hz, 1 H), 3.05 (dd, *J* = 14, 8.0 Hz, 1 H). <sup>19</sup>F NMR (D<sub>2</sub>O); δ -137 (m, 1 F). HRMS calcd. for C<sub>9</sub>H<sub>10</sub>NO<sub>3</sub>F (MH)<sup>+</sup>, 200.0723; found, 200.0721.

**2,6-Difluorotyrosine (4).** <sup>1</sup>H NMR (D<sub>2</sub>O); δ 6.22 (m, 2 H), 3.67 (m, 1 H), 3.01 (dd, *J* = 14.8, 6.0 Hz, 1 H), 2.88 (dd, *J* = 14.8, 8.0 Hz,

1 H). <sup>19</sup>F NMR (D<sub>2</sub>O); δ -116 (s, 2 F). HRMS calcd. for C<sub>9</sub>H<sub>9</sub>NO<sub>3</sub>F<sub>2</sub> (MH)<sup>+</sup>, 218.0629; found, 218.0630.

**2,3-Difluorotyrosine (5).** <sup>1</sup>H NMR (D<sub>2</sub>O); δ 6.90 (m, 1 H), 6.70 (m, 1 H), 3.95 (dd, *J* = 8.0, 5.2 Hz, 1 H), 3.31 (dd, *J* = 14.8, 5.2 Hz, 1 H), 2.88 (dd, *J* = 14.8, 8.0 Hz, 1 H). <sup>19</sup>F NMR (D<sub>2</sub>O); δ -143 (d, *J* = 18.8 Hz, 1 F), -163 (d, *J* = 18.8 Hz, 1 F). HRMS calcd. for C<sub>9</sub>H<sub>9</sub>NO<sub>3</sub>F<sub>2</sub> (MH)<sup>+</sup>, 218.0629; found, 218.0629.

**2,5-Difluorotyrosine (6).** <sup>1</sup>H NMR (D<sub>2</sub>O); δ 7.03 (dd, *J* = 11.2, 7.6 Hz, 1 H), 6.71 (dd, *J* = 11.2, 7.6 Hz, 1 H), 3.95 (dd, *J* = 8.0, 5.3 Hz, 1 H), 3.26 (dd, *J* = 14.8, 5.3 Hz, 1 H), δ 3.03 (dd, *J* = 14.8, 8.0 Hz, 1 H). <sup>19</sup>F NMR (D<sub>2</sub>O); δ -123 (m, 1 F), -143 (m, 1 F). HRMS calcd. for C<sub>9</sub>H<sub>9</sub>NO<sub>3</sub>F<sub>2</sub> (MH)<sup>+</sup>, 218.0629; found, 218.0627.

**3,5-Difluorotyrosine (7).** <sup>1</sup>H NMR (D<sub>2</sub>O); δ 6.85 (m, 2 H), 3.93 (dd, *J* = 8.4, 4.5 Hz, 1 H), 3.20 (dd, *J* = 14.8, 4.5 Hz, 1 H), 2.88 (dd, *J* = 14.8, 8.4 Hz, 1 H). <sup>19</sup>F NMR (D<sub>2</sub>O); δ -135 (brs, 2 F). HRMS calcd. for C<sub>9</sub>H<sub>9</sub>NO<sub>3</sub>F<sub>2</sub> (MH)<sup>+</sup>, 218.0629; found, 218.0631.

**2,3,6-Trifluorotyrosine (8).** <sup>1</sup>H NMR (D<sub>2</sub>O); δ 6.24 (m, 1 H), 3.71 (brs, 1 H), 3.07 (d, *J* = 14.8 Hz, 1 H), 2.92 (m, 1 H). <sup>19</sup>F NMR (D<sub>2</sub>O); δ -124 (m, 1 F), -143 (m, 1 F), -169 (m, 1 F). HRMS calcd. for C<sub>9</sub>H<sub>8</sub>NO<sub>3</sub>F<sub>3</sub> (MH)<sup>+</sup>, 236.0535; found, 236.0538.

**2,3,5-Trifluorotyrosine (9).** <sup>1</sup>H NMR (D<sub>2</sub>O); δ 6.58 (brs, 1 H), 3.70 (brs, 1 H), 3.10 (d, *J* = 14.4 Hz, 1 H), 2.85 (t, *J* = 7.2 Hz, 1 H). <sup>19</sup>F NMR (D<sub>2</sub>O); δ -151 (m, 1 F), -158 (m, 1 F), -170 (m, 1 F). HRMS calcd. for C<sub>9</sub>H<sub>8</sub>NO<sub>3</sub>F<sub>3</sub> (MH)<sup>+</sup>, 236.0535; found, 236.0535.

**2,3,5,6-Trifluorotyrosine (10).** <sup>1</sup>H NMR (D<sub>2</sub>O); δ 3.92 (m, 1 H), 3.27 (m, 1 H), 3.16 (m, 1 H). <sup>19</sup>F NMR (D<sub>2</sub>O); δ -150 (m, 2 F), -167 (m, 2 F). HRMS calcd. for C<sub>9</sub>H<sub>7</sub>NO<sub>3</sub>F<sub>4</sub> (MH)<sup>+</sup>, 254.0440; found, 254.0441.

**Measurements of Fluorotyrosine Analogue pK<sub>a</sub> Values.** The pK<sub>a</sub> values of the fluorotyrosine analogues were determined spectrophotometrically by monitoring the bathochromic shift (ca. 270 nm → 290 nm) that occurs upon conversion of the neutral phenol to the phenoxide anion. Appropriate pH ranges (3–11) for each analogue were obtained using the following buffers (30 mM): formate, acetate, Mes, Mops, Tris, Caps, and Caps along with 150 mM NaCl at 30 °C. Data were fit to the Hill equation, demonstrating a single proton-transfer titration, and standard errors for calculated pK<sub>a</sub> values were ±0.2 unit. Previous work has shown that there is good agreement (±0.3 unit) between phenol pK<sub>a</sub> values of the free amino acids and peptides.<sup>24</sup>

**Synthesis of Fmoc-fluorotyrosine Analogues. General.** The fluorotyrosine analogue (1 mmol) was dissolved in 10% w/w aqueous sodium carbonate (10 mL), and a solution of 9-fluorenylmethyl *N*-succinimidyl carbonate (0.337 g, 2 mmol) in dioxane (5 mL) was added dropwise while stirring the mixture at room temperature. Subsequently, the reaction mixture was poured into water (50 mL) and extracted with diethyl ether (2 × 100 mL). The aqueous phase was acidified while being vigorously stirred with concentrated HCl to reach pH 3, and then the aqueous phase was extracted with ethyl acetate (100 mL). The organic phase was dried over anhydrous MgSO<sub>4</sub>, and the solvent was removed in vacuo. The Fmoc derivative whose identity was verified by TLC and NMR was used in peptide synthesis without further purification.

**Synthesis of Heptapeptides Containing Fluorotyrosine Analogues.** Heptapeptides (EDNEXTA) with X = tyrosine analogues 1–10 were synthesized by automated Fmoc solid-phase peptide synthesis on a 0.1–0.25 mmol scale using the unprotected Fmoc-fluorotyrosine analogues generated above. The peptides were purified on a C-18 reverse phase column using a linear gradient (acetonitrile/water containing 0.05% v/v trifluoroacetic acid) and then were lyophilized to dryness. The molecular weight of each heptapeptide was confirmed using electrospray mass spectrometry, and purity (>95%) was determined by analytical HPLC.

**Profiles of pH versus Rate for Csk-Catalyzed Phosphorylation of the Heptapeptide Family EDNEXTA (X = 1, 6, 8–10).** Kinase assays were performed using the spectrophotometric coupled assay that monitors ADP formation with minor modifications of previously described procedures.<sup>24</sup> Briefly, reactions contained 60 mM buffer, 15 mM MgCl<sub>2</sub>, 1 mM ATP, 190 μM NADH, 1 mM phosphoenolpyruvate, excess pyruvate kinase and lactate dehydrogenase, and pure recombinant Csk. At least five different peptide substrate concentrations in the range of 1–16 mM were used, and duplicate assays gave rate

(29) Chen, H.; Gollnick, P.; Phillips, R. S. *Eur. J. Biochem.* **1995**, *229*, 540–549.

constants within 20%. Turnover of the limiting substrate was not allowed to exceed 10%. Data were fit to the Michaelis–Menten equation using a nonlinear curve fit, which in a number of cases only allowed accurate  $k_{\text{cat}}/K_{\text{m}}$  values to be obtained because the  $K_{\text{m}}$  values were larger than 10 mM. Buffers used were Bis-Tris for pH 6.0–6.3, Mops for pH 6.3–7.5, and Tris for pH 7.5–8.6. Although at pH 7.5, an overlap point for Mops and Tris, the  $k_{\text{cat}}/K_{\text{m}}$  with Mops tended to be higher (1.2–2-fold) than with Tris for the various peptide substrates; normalization did not lead to a significant impact on the calculated acidity constants. Enzyme activity was stable (<10% activity loss) over all pH values used in this study for at least 5 min. Reactions were initiated with Csk, and reaction rates were linear for at least 5 min at all pH values. Plots of  $\log(k_{\text{cat}}/K_{\text{m}})_{\text{app}}$  vs pH for EDNEYTA were fit to:

$$\log(k_{\text{cat}}/K_{\text{m}})_{\text{app}} = \log(\{k_{\text{cat}}/K_{\text{m}}\}/[1 + H/K_1])$$

where  $H$  is the proton concentration and  $K_1$  is the dissociation constant for the ionizable group that is active when deprotonated. For EDNEXTA where  $X$  = fluorotyrosine analogue, the equation used was

$$\log(k_{\text{cat}}/K_{\text{m}})_{\text{app}} = \log(\{k_{\text{cat}}/K_{\text{m}}\}/[1 + H/K_1 + K_2/H])$$

where  $H$  is the proton concentration,  $K_1$  is the dissociation constant for the ionizable group that is active when deprotonated, and  $K_2$  is the dissociation constant for the ionizable group that is active when protonated. Fits employed the nonlinear least squares approach in the Kinasyst II (Intellikinetix) software package, and dissociation constants  $\pm$  standard errors are shown in Figure 4. The calculated pH-independent values of  $k_{\text{cat}}/K_{\text{m}}$  were associated with significant standard errors (>50%) for peptides containing fluorotyrosine analogues **8–10**. This error along with the decreased number and more limited spread of data points prohibited an accurate determination of the  $\beta_{\text{nuc}}$  using these pH-independent  $k_{\text{cat}}/K_{\text{m}}$  values. In any event, the  $\beta_{\text{nuc}}$  that could be estimated using these data was near 0 as previously determined.

**Preparation of *O*-Phosphofluorotyrosine Heptapeptides.** The 10 different *O*-phosphofluorotyrosine peptides were prepared by large-scale enzymatic phosphorylation of peptides EDNEXTA ( $X = \mathbf{1–10}$ ) with Csk. The standard reaction conditions on a 1-mL scale included the following: 60 mM Tris-HCl, pH 7.4; 3 mM ATP; 3 mM phosphoenolpyruvate; 3 mM MnCl<sub>2</sub>; 1 mM peptide; 5 mM DTT; 10  $\mu\text{g}$  PK-LDH (3:1 pyruvate kinase–lactate dehydrogenase, Boehringer Mannheim); and 1  $\mu\text{M}$  Csk at 30 °C. For the peptide containing tetrafluorotyrosine (**10**), the reaction was done using MOPS–Na buffer, pH = 6.6, with 3  $\mu\text{M}$  Csk. Reactions were followed by analytical reverse-phase HPLC and generally stopped after 48 h where 60–90% conversion was observed. Approximately, 30 1-mL reactions were performed in parallel for each peptide. Purification of phosphorylated peptides (>95%) was accomplished using reverse-phase HPLC with a

C-18 column using a linear gradient of acetonitrile–water containing 0.05% trifluoroacetic acid. Unphosphorylated peptides showed retention times of approximately 24 min and phosphorylated peptides retention times of approximately 16 min. The molecular composition of phosphopeptides was confirmed using electrospray mass spectrometry.

**Reverse Kinase Assays.** The general procedure involved a direct HPLC assay monitoring of the conversion of phosphopeptide to dephosphopeptide. Using this approach, the lower limit of detection of the conversion of peptide to dephosphorylated peptide was 0.5% turnover. Standard reaction conditions were performed with 60 mM Tris-HCl, pH 7.4, 12 mM MgCl<sub>2</sub>, 1 mM ADP, and 1 mM DTT at 30 °C in 40  $\mu\text{L}$ . A 20- $\mu\text{L}$  aliquot was diluted with 40  $\mu\text{L}$  of water, and the sample was injected onto an HPLC (C-18 column) with flow rate 1 mL/min using a linear gradient (acetonitrile–H<sub>2</sub>O with 0.05% trifluoroacetic acid) as above with UV monitoring at 214 nm. Peak areas of peptides were determined by integration using the Rainin software package and referenced against standard amounts of pure materials. The true reverse kinase activity was obtained by subtracting (where necessary) the rate of phosphoryl transfer in the absence of ADP from the total rate (in the presence of ADP). Subtraction proved to be necessary for peptides with fluorotyrosine analogues **1**, **2**, **7**, and **8**, which had reproducible background rates of 40%, 70%, 60%, and 40% of the total rates, respectively. However, the overall slope in Figure 6 ( $-0.33 \pm 0.06$ ) was not significantly affected by omission of these correction factors ( $-0.27 \pm 0.05$ ) or by complete omission of the points with high backgrounds ( $-0.38 \pm 0.05$ ). For all other peptides, the background rates were <15% of the total rates. All rate measurements were performed at least three times, and repeat measurements gave rates within 20% of each other. Reactions were shown to display linear activity for at least 60 min, and activity was linear with respect to Csk enzyme concentration in the 1–10  $\mu\text{M}$  range. Reaction rates were linear with respect to phosphopeptide concentration range (1–4 mM) for all phosphopeptides so that only  $k_{\text{cat}}/K_{\text{m}}$  results are plotted. Initial conditions were used for all rate measurements with less than 10% turnover of the limiting substrate.

**Acknowledgment.** Support from the Damon Runyon Scholar Award Program, the NIH (CA 74305-01), the Irving Hansen Foundation, and the Monique Weill-Caulier Trust is gratefully acknowledged. We thank R. Phillips for the tyrosine phenol-lyase overproducing strain and helpful advice. We thank A. S. Mildvan for helpful suggestions and a critical evaluation of the manuscript.

JA9808393